

폴리염화비닐의 광안정성 향상에 대한 ZnO/키토산 나노복합체의 시너지 효과

Nibras Abdul-Ameer Aboud, Khawla Kareem*, Ali J. Al-Sarray**,[†] Basma Esam Jasim,
Shaimaa B. Al-baghdadi***, and Ahmed A. Ahmed**

Department of Chemical Industrial, Institute of Technology/Baghdad, Middle Technical University

*Ministry of Education, Directorate of Rusafa-2, Baghdad, Iraq

**Polymer Research Unit, College of Science, Mustansiriyah University

***Energy and renewable Energies Technology Center, University of Technology-Iraq

(2024년 10월 28일 접수, 2024년 12월 6일 수정, 2024년 12월 8일 채택)

Synergistic Effect of ZnO/Chitosan Nanocomposite on the Photostability Enhancement of Polyvinyl Chloride

Nibras Abdul-Ameer Aboud, Khawla Kareem*, Ali J. Al-Sarray**,[†] Basma Esam Jasim,
Shaimaa B. Al-baghdadi***, and Ahmed A. Ahmed**

Department of Chemical Industrial, Institute of Technology/Baghdad, Middle Technical University, 10074 Iraq

*Ministry of Education, Directorate of Rusafa-2, Baghdad, 10064 Iraq

**Polymer Research Unit, College of Science, Mustansiriyah University, 10052 Iraq

***Energy and renewable Energies Technology Center, University of Technology, 10066 Iraq

(Received October 28, 2024; Revised December 6, 2024; Accepted December 8, 2024)

Abstract: This study investigates the enhancement of poly(vinyl chloride) (PVC) properties through the incorporation of zinc oxide (ZnO) nanoparticles and chitosan to improve its resistance to UV-induced photodegradation. The nanocomposites were synthesized by blending ZnO and chitosan with PVC, followed by comprehensive characterization using X-ray diffraction (XRD), field emission scanning electron microscopy (FE-SEM), atomic force microscopy (AFM), and Fourier transform infrared (FTIR). XRD confirmed the crystalline structure of ZnO-chitosan nanoparticles with a crystal size of 25.38 nm, while FE-SEM analysis revealed an average grain size of 76.68 nm, indicating the successful formation of nanoscale materials. AFM demonstrated a significant reduction in surface roughness and photodegradation in the nanocomposite films compared to pure PVC. FTIR analysis revealed lower photodegradation indices (IPO, ICO, IOH) in the nanocomposites across UV irradiation durations of 0, 50, 100, 150, 200, 250, and 300 h, indicating a delayed formation of carbonyl and hydroxyl groups. Weight loss and viscosity measurements further confirmed enhanced UV stability, attributed to the synergistic effect of ZnO's UV-shielding properties and chitosan's radical-scavenging capabilities. These results highlight the potential of ZnO-chitosan nanocomposites to significantly extend the service life of PVC in harsh environments.

Keywords: nanocomposites, poly(vinyl chloride), photodegradation of poly(vinyl chloride), zinc oxide, chitosan.

Introduction

Poly(vinyl chloride) (PVC) is a widely used thermoplastic polymer valued for its versatility and cost-effectiveness. It is commonly employed in a variety of applications, including flexible plastics, molded products, pipes, cables, siding, foils, and

films. Despite its widespread use, PVC exhibits lower thermal stability compared to polymers such as polyethylene (C_2H_4)_n, polypropylene (C_3H_6)_n, and polystyrene (C_8H_8)_n.¹⁻³ This thermal instability is primarily attributed to the presence of weak Carbon-Chlorine (C-Cl) and Carbon-Hydrogen (C-H) bonds, as well as defects within the polymer chains.⁴⁻⁶ PVC's high chlorine content further contributes to its degradation through dehydrochlorination, leading to the formation of conjugated polyene structures when exposed to heat. Consequently, PVC becomes susceptible to degradation under thermal and UV stress, lim-

[†]To whom correspondence should be addressed.
ali_alsarray@uomustansiriyah.edu.iq, ORCID[®] 0000-0001-6484-1763
©2025 The Polymer Society of Korea. All rights reserved.

iting its performance in high-temperature environments.^{7,8}

Recent research has focused on improving the thermal stability of PVC by incorporating various additives and fillers to enhance its resistance to dehydrochlorination, increase its mechanical properties, and extend its service life. These additives, particularly inorganic nanomaterials, play a crucial role in improving the thermal, mechanical, and chemical properties of PVC.⁵ Among these, zinc oxide (ZnO) has been extensively studied due to its exceptional thermal stability, low dielectric constant, and desirable optical and antimicrobial properties.⁹⁻¹¹ ZnO nanoparticles, with their high specific surface area and strong interfacial bonding with the polymer matrix, have shown promise in enhancing PVC's overall stability and resistance to UV-induced degradation.¹²

In addition to inorganic additives, biopolymeric materials such as chitosan have attracted significant attention as potential enhancers of PVC properties. Chitosan is a natural polysaccharide derived from chitin, which is commonly found in the exoskeletons of crustaceans and the cell walls of fungi.¹³⁻¹⁵ Structurally, chitosan is composed of 2-amino-2-deoxy- β -D-glucose units linked by 1,4-glycosidic bonds.¹⁶ Due to its biocompatibility, biodegradability, and intrinsic antimicrobial properties, chitosan has been widely utilized in various biomedical and environmental applications,¹⁶ including drug delivery systems,¹² wound dressings, and packaging materials.^{17,18}

Recent studies have explored the development of PVC nanocomposites incorporating both ZnO and chitosan to enhance the thermal, mechanical, and antimicrobial properties of the polymer.¹² The combination of ZnO and chitosan is particularly attractive for applications in medical and packaging fields, where improved stability and antimicrobial resistance are crucial. This study aims to investigate the effect of ZnO and chitosan-based additives on the photodegradation resistance and overall performance of PVC films, with a focus on extending the polymer's lifespan and functionality in challenging environments.

Experimental

Materials. Without further purification, all compounds were analytical reagent grades purchased from Sigma-Aldrich.

Synthesis of ZnO/Chitosan Nanoparticles. A nanocomposite of chitosan and zinc oxide was synthesized. According to the previously conducted method,¹² sodium hydroxide served as the oxidizing agent and sodium tripolyphosphate (STPP) served as the cross-linking agent. Typically, the reaction began

at 25 °C by adding the basic reactants, where 35 mL of distilled water was mixed with 1 gram of chitosan and 1.5 mmol $\text{Zn}(\text{NO}_3)_2 \cdot 6\text{H}_2\text{O}$. 2.5 mL of acetic acid was then added to the composition which was stirred at 500 rpm until a transparent and uniform viscose solution was produced. The mixture was then gradually dropped into a 400 mL aqueous solution containing STPP (4 g) and NaOH (3.2 g), raising the pH of the mixture to 10. For approximately 3 h, the mixture is placed in a water bath at a temperature ranging from (40 to 80 °C), The solution product was separated, washed several times with deionized water, precipitated, then dried at 60 °C for 7 h. The synthesis yielded approximately 85% of a white nanocomposite complex.¹⁹

Modified Polymeric Film Synthesis. PVC (5 g) was dissolved in 100 mL of tetrahydrofuran (THF) without and with the addition of the nanocomplex ZnO/chitosan (0.025 g) and stirred for 2 h at 25 °C. The concentration of ZnO/chitosan was selected in order to balance UV stability, mechanical integrity, and ease of film casting. Dishes were prepared for casting solutions by repeatedly washing the dish used in the film casting process with THF and drying it for 48 h at 25 °C. The casting process is then carried out at 25 °C, where the films are created by evaporation.²⁰

Photodegradation Measuring Methods. The photodegradation of polyvinyl chloride (PVC) films was evaluated after exposure to radiation in the 250–380 nm range using a QUV accelerated weatherometer in the Polymer Research Unit. The high-temperature conditions simulated prolonged UV exposure to assess the effectiveness of the additives in enhancing PVC's photostability.

Photodegradation Measuring Methods: The stabilization efficiency of the additives was evaluated by comparing the weight loss percentages of photodegraded PVC films, both with and without additives, using eq. (1).^{21,22}

$$\text{Weight loss percentage} = \frac{W_1 - W_2}{W_1} \times 100 \quad (1)$$

where W_1 is the weight of the sample before irradiation and W_2 is the weight of the sample after irradiation.

FTIR Spectra: Fourier transform infrared (FTIR) spectroscopy was used to monitor the degree of photodegradation in the PVC films. The spectra were collected using FTIR spectroscopy (JASCO-FT/IR-6X, 7800–350 cm^{-1} , resolution: 0.25 cm^{-1}) in the Polymer Research Unit, with the degradation process being tracked by observing changes in specific peak intensities over time. Photodegradation indices were calculated by

comparing the absorbance of peaks at 1631, 1724, and 3400 cm^{-1} to a reference PVC peak, according to eq. (2).^{23,24}

$$I_s = \frac{A_s}{A_r} \quad (2)$$

where I_s is the degradation index for the studied groups, A_s is the absorbance of the investigated peak, and A_r is the absorbance of the reference peak.

Average Molecular Weight (M_w) by Viscosity: The average molecular weight (M_w) of PVC films (40 μm thickness) was determined by dissolving the films in tetrahydrofuran (THF) at 25 $^\circ\text{C}$. Films were either blank or contained 0.02 wt.% of the ZnO/chitosan complex and were exposed to UV light with an absorption intensity of 6.02×10^{-9} $\text{ein dm}^{-3}\text{s}^{-1}$. The molecular weight was calculated using the Mark-Houwink equation (eq. 3).^{1,25}

$$[\eta] = K(\overline{Mv})^\alpha \quad (3)$$

where K and α are constants dependent on the polymer-solvent system and temperature, whereas $[\eta]$ represents intrinsic viscosity, while \overline{Mv} is the average molecular weight.

Results and discussion

XRD Analysis. The X-ray diffraction (XRD) pattern of the ZnO/chitosan nanostructures is presented in Figure 1. Strong and distinct diffraction peaks were observed at 2θ values of 31.6° , 34.36° , and 36.39° , corresponding to the (100), (002), and (101) planes, respectively, which are characteristic of ZnO (JCPDS card no. 36-1451). These peaks confirm the crystalline structure of ZnO in the composite. In addition to the ZnO peaks,

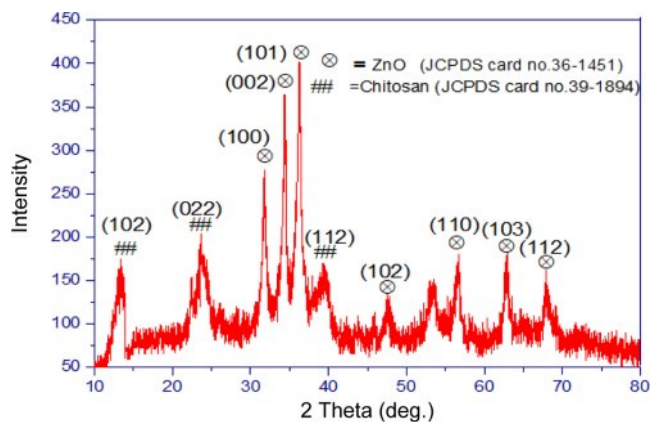


Figure 1. XRD pattern of ZnO/chitosan nanostructures.

diffraction peaks at 2θ values of 13.30° , 23.68° , and 39.34° were observed, corresponding to the (102), (022), and (112) planes, respectively. These peaks are attributed to the chitosan phase, as confirmed by the JCPDS card no. 39-1894 (6) (20) and supported by literature data. The crystallite size of the ZnO nanoparticles within the chitosan matrix was estimated using the Debye-Scherrer equation (eq. 4).

$$D = \frac{k\lambda}{\beta \cos \theta} \quad (4)$$

where D is crystallite size, k is shape factor (0.9), λ is wavelength of X-ray (0.1406 nm), β is full width at half maximum (FWHM), and θ is Bragg diffraction angle.

The average crystallite size of the ZnO nanostructures was found to be approximately 18.24 nm. This nanoscale size contributes to the enhanced properties of the ZnO/chitosan composite material.

FE-SEM Analysis. Field emission scanning electron microscopy (FE-SEM) images were obtained using a Zeiss instrument at the University of Tehran, Iran. Figure 2 shows the FE-SEM image of the ZnO/chitosan nanocomposite. The image reveals that the sample exhibited a spherical morphology with uniform particle distribution and minor aggregation. Agglomeration was attributed to crystal interactions, leading to the formation of agglomeration voids of varying sizes. The average grain size was measured using the FE-SEM image analysis tool and was found to be approximately 20.45 nm. This result aligns well with the particle size calculated from the XRD analysis, confirming the successful synthesis and preparation of the nanocomposite.

AFM Analysis. Atomic force microscopy (AFM) was used to assess the surface morphology of both pure PVC and PVC

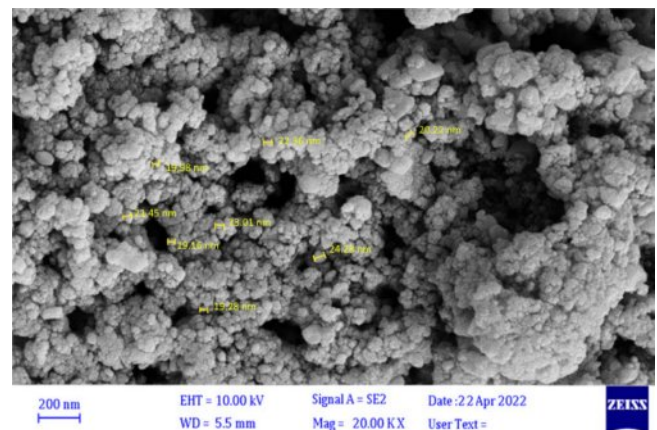


Figure 2. FE-SEM image of the prepared ZnO/chitosan nanocomposite.

incorporated with ZnO/chitosan nanoparticles after 300 h of UV irradiation. The AFM images reveal that pure PVC (Figure 3(a)) exhibits significant surface roughening, with a root mean square roughness (S_q) of 6.9 nm and a peak-to-peak height (S_z) of 53.19 nm. These features indicate considerable degradation due to photodegradation, characterized by chain scission and surface irregularities. In contrast, the ZnO/chitosan-incorporated PVC (Figure 3(b)) shows a more controlled surface morphology, with a slightly higher S_q of 7.39 nm but a smoother overall surface, as indicated by a peak-to-peak height (S_z) of 71.47 nm. The presence of ZnO nanoparticles, known for their UV-absorbing properties, effectively reduced the extent of surface degradation, as seen in the lower roughness and more uniform structure.

Additionally, the fractal dimension increased from 2.65 in pure PVC to 2.78 in the nanoparticle-incorporated PVC, indicating a more complex and stable surface. These findings suggest

that ZnO/chitosan nanoparticles enhance the photostability of PVC by mitigating UV-induced degradation and preserving surface integrity. The nanoparticles act as a UV shield, while chitosan adds mechanical stability, preventing excessive roughening.^{26,27}

Modified Polymeric Film Characterization. Weight Loss Technique: The results indicate that ZnO/chitosan nanoparticles exhibit a photo-stabilizing effect on PVC samples, resulting in a significant reduction in weight loss percentage compared to blank PVC, as shown in Figure 4.

FTIR Analysis According to Functional Groups' Indices: The FTIR spectra of the films were recorded at a wavelength of 225 nm. Bands at 1772 cm^{-1} and 1724 cm^{-1} correspond to carbonyl groups, specifically from chloroketone and aliphatic ketone, respectively. The carbonyl absorption bands appear at 1770 and 1724 cm^{-1} , while polyene structures with various conjugated bonds were identified through reference absorption

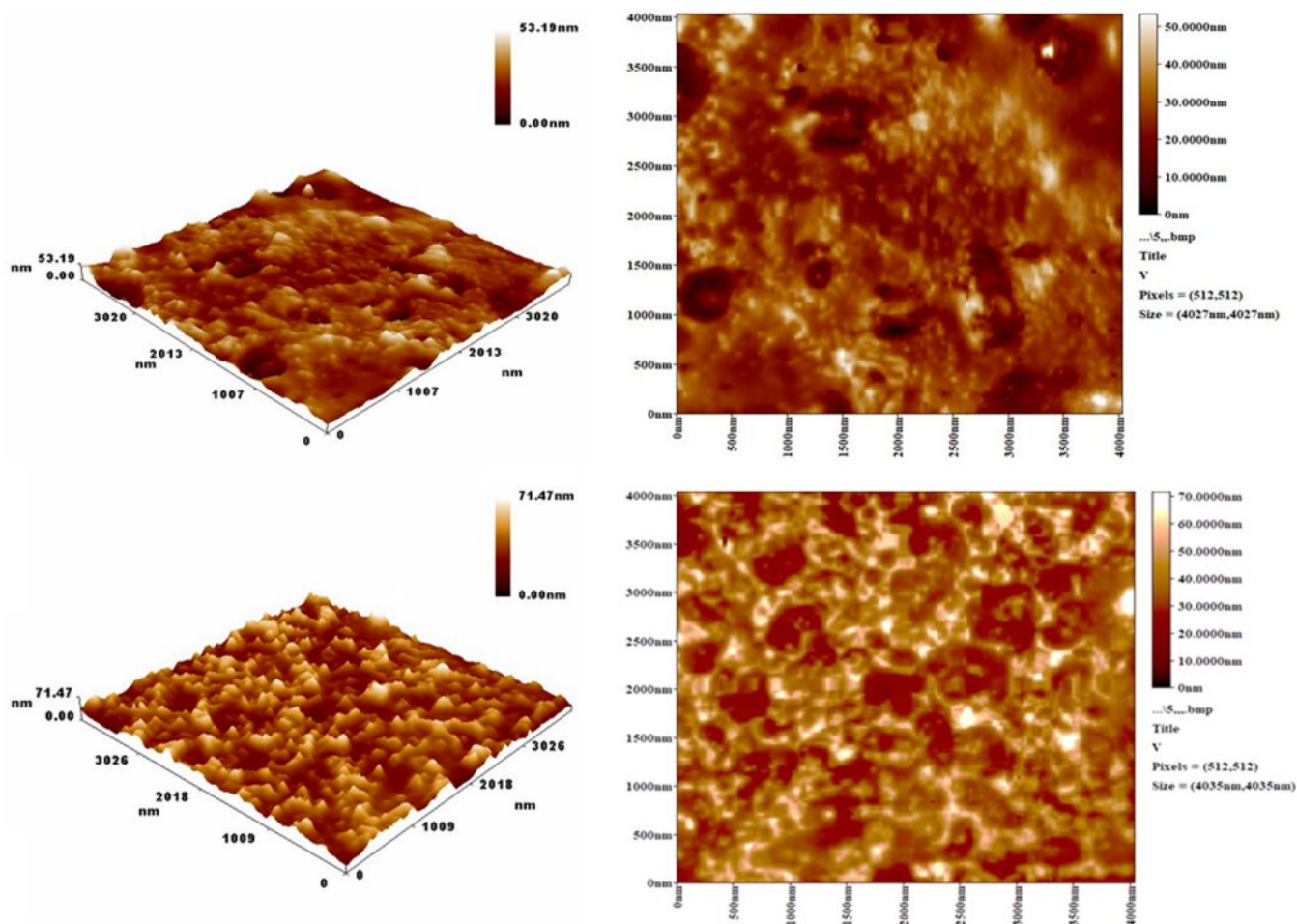


Figure 3. AFM surface morphology of (a) pure PVC; (b) ZnO/Chitosan nanoparticle-incorporated PVC after UV irradiation for 300 h.

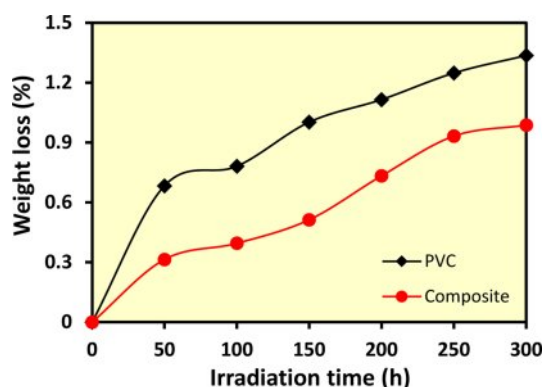


Figure 4. Weight loss of PVC films with and without additive under photodegradation conditions.

energies at 1631 and 3400 cm^{-1} . The OH band observed at 3500 cm^{-1} is attributed to alcohol functionality, indicating that the modified polymers act as PVC stabilizers. Additionally, the 1722 cm^{-1} peak corresponds to the aliphatic ketone, and the 1602 cm^{-1} peak is associated with a conjugated double bond from the carbonyl group. The hydroxy group at 3500 cm^{-1} , along with polyene, alcohol, and carbonyl groups, were analyzed to investigate the photodegradation process of PVC films in the presence of the nanocomplex.

The I_{PO} value of PVC (calculated from irradiated polyvinyl chloride/CH-ZnO films) increased with irradiation time as illustrated in Figure 5(a), indicating that the additives function as optical stabilizers, reducing photocatalytic degradation. This was evidenced by the decrease in the I_{CO} value, particularly when compared to pure PVC films, which suggests that ZnO acts as an effective UV absorber, reducing photodegradation by preventing the formation of free radicals. Simultaneously, chitosan contributes by scavenging existing free radicals, thus further limiting the degradation process. As the irradiation time increased from 0 to 300 minutes, the carbonyl (I_{CO}) (Figure 5(b)) and hydroxyl (I_{OH}) coefficients (Figure 5(c)) increased, though the complex additives exhibited better photostability than pure PVC.

Molecular Weight (M_w) Variation of PVC Films during Photolysis: Figure 6. shows the variation in molecular weight (M_w) and viscosity of PVC films incorporating 0.02% w/v ZnO/chitosan nanoparticles as an additive. The results indicate that weak links in the polymer chains lead to a rapid decrease in molecular weight during photolysis. Pure PVC films experienced a more significant drop in molecular weight compared to PVC films modified with the additive, suggesting that ZnO/chitosan provides enhanced optical and polymeric stability. This stabilization

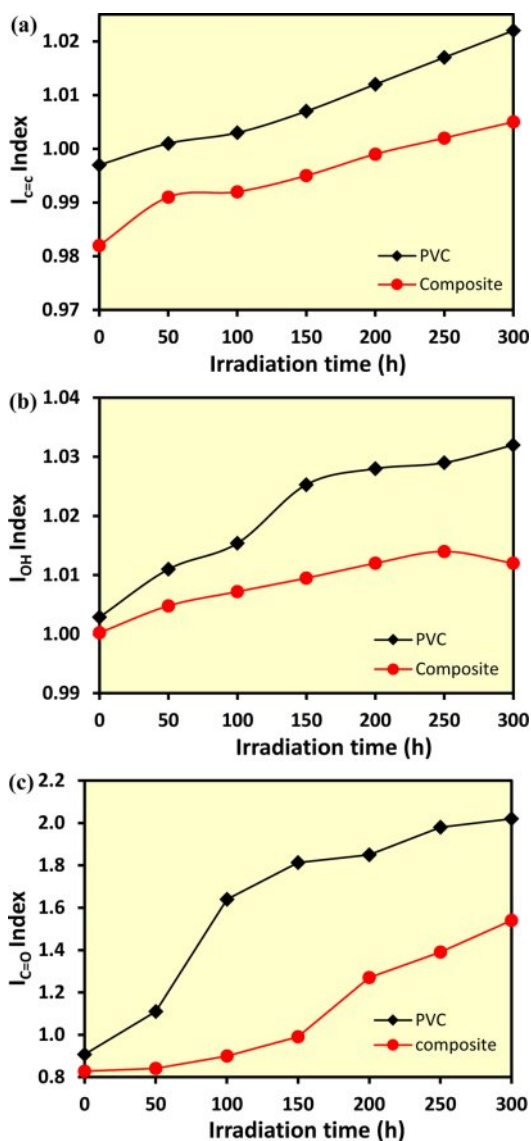


Figure 5. Variation of (a) I_{PO} ; (b) I_{CO} ; (c) I_{OH} indices as a function of irradiation time for PVC with and without additive.

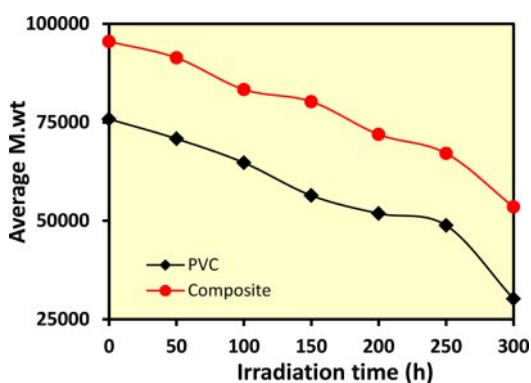


Figure 6. Variation of viscosity average molecular weight (M_v) of PVC films with 0.02% w/v ZnO/chitosan as additives.

effect prevents polymer degradation, particularly at the chain ends where free radicals could otherwise increase viscosity. The extent of degradation is closely tied to the irradiation time, with longer exposure accelerating chain breakage.

The data support the hypothesis that polymers can undergo photodegradation-induced chain scission. Crosslinking, evidenced by the presence of non-dissolving material, leads to increased chain scission rates and reduces molecular weight as polymer breakdown progresses. Hydrolyzed polymers show a more significant molecular weight decrease due to chain scission compared to unhydrolyzed polymers. The random breaking of weak links within the polymer chains during photolysis results in a rapid increase in radioactivity, highlighting the random degradation process.²⁶

The study tracked the viscous molecular weight ratio, polymer chain scission rate, and the degradation of pure PVC films as well as those modified with the ZnO/chitosan complex. These modified films exhibited minimal sensitivity to light or heat, as the nanoadditives helped preserve the high melting points and low molecular loss (M_n) and weight loss ratio (%). The nanoadditives act as UV absorbers, peroxide scavengers, and radical suppressors, capturing free radicals before they cause damage to the polymer matrix. This improved protection against photolysis is attributed to the better charge dispersion within the polymer facilitated by the nanoparticles, which increase the surface area for UV absorbance. This transition from the polymer's ground state to an excited energy state is described by Jablonski's diagram.²⁷

Conclusions

The present study successfully demonstrated the enhancement of PVC properties by incorporating ZnO nanoparticles and chitosan to form a nanocomposite with improved UV stability. Characterization techniques such as XRD, FE-SEM, and AFM confirmed the nanoscale nature of the ZnO-chitosan particles, with XRD and FE-SEM indicating crystal and grain sizes of 25.38 nm and 76.68 nm, respectively. FTIR analysis highlighted the reduction in photodegradation of the PVC matrix due to the addition of ZnO and chitosan, as evidenced by lower photodegradation indices (I_{PO} , I_{CO} , I_{OH}) across increasing UV irradiation times (0 to 300 h). The results revealed that the nanocomposite exhibited delayed formation of degradation products, thus enhancing its resistance to photo-oxidation. These findings suggest that ZnO-chitosan nanocomposites have strong potential as optical stabilizers and can significantly extend the

service life of PVC in various applications, particularly those exposed to harsh environmental conditions such as UV light.

Acknowledgment: The authors would like to thank Mustansiriyah University (www.uomustansiriyah.edu.iq) Baghdad-Iraq for supporting the present work.

Conflict of Interest: The authors declare that there is no conflict of interest.

References

1. Wilkes, C. E.; Summers, J. W.; Daniels, C. A.; Berard, M. T. *PVC Handbook*; Hanser Munich, 2005.
2. Gupta, V. K.; Singh, A. K.; Mehtab, S.; Gupta, B. A. Cobalt (II)-selective PVC Membrane Based on a Schiff Base Complex of N, N'-bis (salicylidene)-3,4-diaminotoluene. *Anal. Chim. Acta* **2006**, 566, 5-10.
3. Ye, Q.; Ma, X.; Li, B.; Jin, Z.; Xu, Y.; Fang, C.; Zhou, X.; Ge, Y.; Ye, F. Development and Investigation of Lanthanum Sulfadiazine with Calcium Stearate and Epoxidised Soyabean Oil as Complex Thermal Stabilizers for Stabilizing Poly(vinyl chloride). *Polymers* **2019**, 11, 531.
4. Jin, D.; Khanal, S.; Zhang, C.; Xu, S. Photodegradation of Polybenzimidazole/polyvinyl Chloride Composites and Polybenzimidazole: Density Functional Theory and Experimental Study. *J. Appl. Polym. Sci.* **2021**, 138, 49693.
5. Sivalingam, G.; Karthik, R.; Madras, G. Effect of Metal Oxides on Thermal Degradation of Poly(vinyl acetate) and Poly(vinyl chloride) and Their Blends. *Ind. Eng. Chem. Res.* **2003**, 42, 3647-3653.
6. Al-Sarray, A. J. A.; Jasim, B. E.; Aboud, N. A.-A.; Moaen, F. J. Enhancing the Photostability of Poly(Vinyl Chloride)(PVC) Through the Incorporation of Cerium and Samarium Oxide. *Polym. Korea* **2024**, 48, 188-194.
7. Taha, T.; Hendawy, N.; El-Rabaie, S.; Esmat, A.; El-Mansy, M. Effect of NiO NPs Doping on the Structure and Optical Properties of PVC Polymer Films. *Polym. Bull.* **2019**, 76, 4769-4784.
8. Hamud, W. M.; Al-Karawi, A. J. M.; Al-Kinani, E. M.; Al-Sarray, A. J. Removal of Proflavine Sulphate Dye From Wastewater Using Tea-bag Tissue as An Adsorbent. *Desalin. Water Treat.* **2024**, 320, 100613.
9. Patil, A. S.; Patil, A. V.; Dighavkar, C. G.; Adole, V. A.; Tupe, U. J. Synthesis Techniques and Applications of Rare Earth Metal Oxides Semiconductors: A review. *Chem. Phys. Lett.* **2022**, 796, 139555.
10. Mahdi Al-Hassani, R. A.; Al-Sarray, A. J. Synthesis, Characterization, Cytotoxicity, Biological Evaluation, DFT Calculations, and Molecular Docking of a Novel Schiff Base and Its Pt (IV) Complex. *Appl. Organomet. Chem.* **2025**, 39, e70046.
11. Jasim, B. E.; Al-Sarray, A. J.; Dadoosh, R. M. Enhanced Alizarin Removal from Aqueous Solutions Using Zinc Oxide/Nickel Oxide Nano-composite. *Anal. Sci. Technol.* **2024**, 37, 39-46.

12. Yadollahi, M.; Farhoudian, S.; Barkhordari, S.; Gholamali, I.; Farhadnejad, H.; Motasadizadeh, H. Facile Synthesis of Chitosan/ZnO Bio-nanocomposite Hydrogel Beads as Drug Delivery Systems. *Int. J. Biological Macromol.* **2016**, *82*, 273-278.
13. Abdelrazek, E.; Elashmawi, I.; Labeeb, S. Chitosan Filler Effects on the Experimental Characterization, Spectroscopic Investigation and Thermal Studies of PVA/PVP Blend Films. *Physica B: Condensed Matter* **2010**, *405*, 2021-2027.
14. Ali, M. E. A.; Aboelfadl, M. M. S.; Selim, A. M.; Khalil, H. F.; Elkady, G. M. Chitosan Nanoparticles Extracted from Shrimp Shells, Application for Removal of Fe(II) and Mn(II) from Aqueous Phases. *Separation Science and Technology* **2018**, *53*, 2870-2881.
15. Tawfiq, K.; Al Naymi, H. A. S.; Obaid, S. M.; Al-Noor, T. H.; Al-Sarray, A. J. Synthesis, Characterization, Molecular Docking, Cytotoxicity, and Antimicrobial Activity of Schiff Base Ligand and Its Metal Complexes. *Appl. Organometallic Chem.* **2024**, e7781.
16. Li, X.; Zeng, D.; Ke, P.; Wang, G.; Zhang, D. Synthesis and Characterization of Magnetic Chitosan Microspheres for Drug Delivery. *RSC Adv.* **2020**, *10*, 7163-7169.
17. Rostami, N.; Dekamin, M. G.; Valiey, E.; Fanimoghadam, H. Chitosan-EDTA-Cellulose Network as a Green, Recyclable and Multifunctional Biopolymeric Organocatalyst for the One-pot Synthesis of 2-amino-4 H-pyran Derivatives. *Sci. Rep.* **2022**, *12*, 8642.
18. Al-Sarray, A. Advancements in Conjugated Polymer Research: Applications in Organic Photovoltaics and Field Effect Transistors. *Current Chem. Lett.* **2024**, *13*, 207-224.
19. AbdElhady, M. Preparation and Characterization of Chitosan/zinc Oxide Nanoparticles for Imparting Antimicrobial and UV Protection to Cotton Fabric. *Int. J. Carbohydrate Chem.* **2012**, *2012*, 840591.
20. Saraci, F.; Quezada-Novoa, V.; Donnarumma, P. R.; Howarth, A. J. Rare-earth Metal-organic Frameworks: from Structure to Applications. *Chem. Soc. Rev.* **2020**, *49*, 7949-7977.
21. Cho, S.; Choi, W. Solid-phase Photocatalytic Degradation of PVC-TiO₂ Polymer Composites. *J. Photochem. Photobiol. A* **2001**, *143*, 221-228.
22. Hajibeygi, M.; Maleki, M.; Shabani, M.; Ducos, F.; Vahabi, H. New Polyvinyl Chloride (PVC) Nanocomposite Consisting of Aromatic Polyamide and Chitosan Modified ZnO Nanoparticles with Enhanced Thermal Stability, Low Heat Release Rate and Improved Mechanical Properties. *Appl. Surf. Sci.* **2018**, *439*, 1163-1179.
23. Sykora, R. E.; Deakin, L.; Mar, A.; Skanthakumar, S.; Soderholm, L.; Albrecht-Schmitt, T. E. Isolation of Intermediate-Valent Ce(III)/Ce(IV) Hydrolysis Products in the Preparation of Cerium Iodates: Electronic and Structural Aspects of Ce₂(IO₃)₆(OH_x)(x≈0 and 0.44). *Chem. Mater.* **2004**, *16*, 1343-1349.
24. Arunachalam, S.; Kirubasankar, B.; Pan, D.; Liu, H.; Yan, C.; Guo, Z.; Angaiah, S. Research Progress in Rare Earths and Their Composites Based Electrode Materials for Supercapacitors. *Green Energy Environ.* **2020**, *5*, 259-273.
25. Keane, M. A. Catalytic Conversion of Waste Plastics: Focus on Waste PVC. *J. Chem. Technol. Biotechnol.: Int. Res. Proc., Environm. Clean Technol.* **2007**, *82*, 787-795.
26. Hadi, A. G.; Jawad, K.; El-Hiti, G. A.; Alotaibi, M. H.; Ahmed, A. A.; Ahmed, D. S.; Yousif, E. Photostabilization of Poly(vinyl chloride) by Organotin(IV) Compounds Against Photodegradation. *Molecules* **2019**, *24*, 3557.
27. Abd AL-Zahra, A.; Fadel, Z. H.; Al-Sarray, A. J.; Hussein, I. A.; Al-Noor, T. H. Corrosion Inhibition of Carbon Steel C45 Using New Azo Derivative in HCl Solution: Synthesis, Potentiostatic Measurement, and DFT Studies. *Russ. J. Phys. Chem. A* **2024**, *98*, 3202-3211.

Publisher's Note The Polymer Society of Korea remains neutral with regard to jurisdictional claims in published articles and institutional affiliations.